# Short-wavelength soft-x-ray laser pumped in double-pulse single-beam non-normal incidence

D. Zimmer,[1,2,3,*] D. Ros,[1] O. Guilbaud,[1] J. Habib,[1] S. Kazamias,[1] B. Zielbauer,[1,2,4] V. Bagnoud,[2,4] B. Ecker,[2,3,4] D. C. Hochhaus,[2,5,6] B. Aurand,[2,3,4] P. Neumayer,[2,5,6] and T. Kuehl[2,3,4]

[1]*LASERIX-CLUPS, LPGP UMR 8578, Université Paris-Sud 11, F-91405 Orsay, France*

[2]*GSI Helmholtzzentrum für Schwerionenforschung GmbH, D-64291 Darmstadt, Germany*

[3]*Institut für Physik, Johannes Gutenberg–Universität Mainz, D-55099 Mainz, Germany*

[4]*Helmholtz Institut Jena, Friedrich-Schiller Universität, D-07743 Jena, Germany*

[5]*ExtreMe Matter Institute EMMI, GSI Helmholtzzentrum für Schwerionenforschung, D-64291 Darmstadt, Germany*

[6]*Institut für Angewandte Physik, Goethe-Universität Frankfurt am Main, D-60438 Frankfurt am Main, Germany*

(Received 26 January 2010; published 6 July 2010)

We demonstrated a 7.36 nm Ni-like samarium soft-x-ray laser, pumped by 36 J of a neodymium:glass chirped-pulse amplification laser. Double-pulse single-beam non-normal-incidence pumping was applied for efficient soft-x-ray laser generation. In this case, the applied technique included a single-optic focusing geometry for large beam diameters, a single-pass grating compressor, traveling-wave tuning capability, and an optimized high-energy laser double pulse. This scheme has the potential for even shorter-wavelength soft-x-ray laser pumping.

DOI: 10.1103/PhysRevA.82.013803 PACS number(s): 42.55.Vc, 52.50.Jm, 52.70.La, 52.38.Ph

## I. INTRODUCTION

A number of applications, including imaging of biological specimens and diagnostics of dense plasmas, require soft-x-ray lasers with short wavelength and narrow bandwidth. In medical and biological research, especially attractive is the possibility of reaching into the so-called water window, the wavelength range between the *K*-shell absorption edges of carbon and oxygen. A main obstacle for laser-produced-plasma soft-x-ray lasers is the high pump laser energy required for the ionization and the excitation of the lasing transitions in quasi-steady-state soft-x-ray lasers [1–4]. Over recent years, tremendous progress has been achieved toward lowering the necessary pump energy by transient collisional schemes [5–9], achieving 8.8 m lasing [10] and even saturated lasing down to 7.3 nm [11] with still moderate pump energies.

Here, we report on the application of double-pulse single-beam non-normal-incidence pumping, which enables us to achieve—with a much simplified setup—lasing down to a short wavelength of 7.3 nm in the transient collisional excitation scheme of laser-produced-plasma soft-x-ray lasers, as reported by [11]. The approach of [11], which used two separate laser beamlines to interact with the target, was a nontrivial complication, because of the delivery of two beams with large dimensions required by the high pump laser energy. More suitable is the approach of [10], which applied two pulses in one beamline to interact with the target. This concept was adapted, by the combination of the focusing system, which consists of only one 90°-off-axis parabola, together with a traveling-wave matching technique, giving a tremendous reduction in setup complexity compared, for example, to [10,11]. This allowed for the application of double-pulse chirped-pulse amplification (CPA) with a total pump energy up to above 100 J at the laser facility PHELIX [12], enabling short-wavelength soft-x-ray lasing with numerous benefits, that is, enhanced stability, reproducibility, decreased cost, and improved efficiency, compared to previous experiments.

## II. SETUP

The experimental setup shown in Fig. 1 applies a double-pulse single-beam non-normal -incidence pumping geometry. The focusing system consists of a diamond free-formed 90°-off-axis copper parabola with a diameter of 300 mm and a focal length of 1500 mm. The aberrations, produced by a tilt $\Theta$ of 4° off the normal off-axis angle, create the line focus without requiring additional optics. The target is rotated to fit the plane of the line focus, resulting in a total incidence angle $\Omega$ of 17° under which the laser double pulse strikes the target with *s* polarization. This corresponds to an incidence angle to the target surface of 73°, a much higher angle as compared to the geometries for softer-x-ray lasers [13]. The range of incidence angles that can be reached in the geometry of the focusing system applied here allows for higher-electron-density laser absorption. The 17° of incidence on the target results in absorption at $9.2 \times 10^{20}$ cm$^{-3}$ for the pump laser wavelength of 1.054 $\mu$m.

The size of the line focus is ~9.9 mm ×20 $\mu$m, giving irradiances of $\sim 5 \times 10^{13}$ W/cm$^2$ for the prepulse and $\sim 1.5 \times 10^{15}$ W/cm$^2$ for the main pulse, for a total pump laser energy of 40 J. The size and the positioning are controlled via an infrared charge-coupled device (CCD) camera in the 10 Hz low-laser-energy mode. For maximal soft-x-ray laser output, the line is shifted horizontally to the amplifier exit of the target, reducing the total length to ~7.9 mm, which is enough for efficient operation, and probably in the saturated regime. During high-energy-laser shots the focus control is done with an x-ray pinhole camera with filters consisting of 1 $\mu$m of $C_3H_6$ and 20 $\mu$m of Al imaging the full line focus onto the camera chip.

The targets are $10 \times 10$ mm$^2$ samarium slabs polished to the crystalline surface structure. The targets are stored under high-purity inert gas until shortly before they are mounted on the target holder and the chamber is evacuated. For each shot

*d.zimmer@gsi.de

 

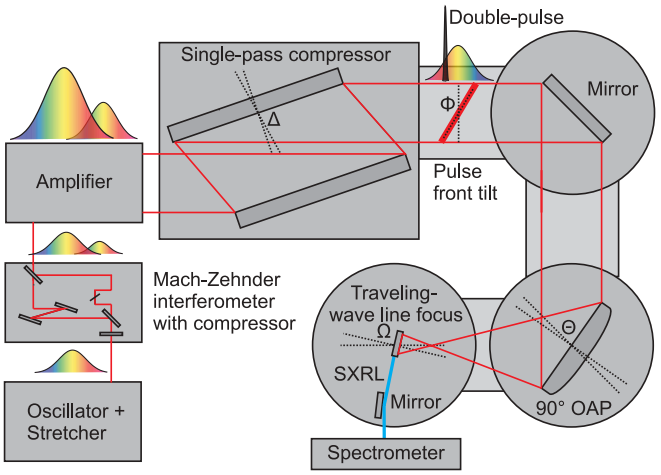


FIG. 1. (Color online) Experimental setup showing the double-pulse generation, the pulse front tilt control, the focusing geometry, and the x-ray laser diagnostic.

a new target position is chosen, far enough from the previous position to be free from the debris created by target ablation. With the given target size, typically 4–5 shots can be placed on one target.

The tuning of the traveling-wave speed is done by rotation of the second grating of the two-grating compressor, thereby changing the pulse front tilt, as in [14]. Tilting the grating introduces a different path length for each point along the beam horizontal axis according to $\Phi(\omega) = \Delta \frac{\omega}{c} \frac{x}{\cos(\Theta_i)\sin(\Theta_r)}[1 + \cos(\Theta_i - \Theta_r)]$, where $x$ is the extension of the beam along the horizontal axis, $\Delta$ is the grating tilt angle, and $\Theta_i$ and $\Theta_r$ are the incident and diffracted angles at the pulsation $\omega$ in the case of the aligned compressor. This equation shows that a spatially dependent additional phase term is added to the pulse, meaning that the compression is not spatially uniform. However, one can show that, when the beam is large compared to the spectral spread on the grating, the increase in pulse duration at the edge of the beam is minimal. For instance, a 0.17° grating tilt yields a 30 ps delay at the focus when a 12 cm beam is used, but at the expense of an increase of pulse duration by 250 fs at the edge of the beam only. During the alignment phase, a test plate with two holes separated by 10 mm is located at the target plane. The two beams are then focused into a nonlinear crystal where second harmonic light is generated. A double pulse of two 1 ps pulses is used at this point to control the amount of pulse front tilt introduced by the compressor. In practice, this corresponds to turning the grating in the compressor until the delay necessary for getting a traveling-wave speed of $1c$ along the line focus is reached, which equals 33 ps or a distance of 10 mm on the delay stage of the double-pulse setup; an autocorrelation mechanism. In this way the intrinsic traveling-wave speed of $2c$ of the line focus is compensated to $(1 \pm 0.1)c$.

The CPA double pulse applied in this pumping scheme consists of two optimized pulses. The first one in the 100 ps regime creates a preplasma in which the energy of the second one in the picosecond regime is deposited. The strong dependence of the soft-x-ray laser performance on the pump laser parameters is known, and therefore it is necessary to control the pump pulses precisely.

To generate an optimized double pulse with variable energy ratio, adjustable time delay, and different pulse durations, a Mach-Zehnder-interferometer-like setup is installed in the front end of the CPA laser system. The stretched oscillator pulse with a group delay dispersion of 200 ps/nm is distributed into two arms via the combination of a $\lambda/2$ wave plate and a polarizing beam splitter to create two pulses with an adjustable energy ratio. The delay between the pulses is controlled between 0 and 3 ns by a delay line placed in one of the arms of the Mach-Zehnder interferometer arrangement. In the other arm, used to prepare the prepulse, a double-pass grating compressor is installed. This compressor changes the group dispersion delay of the prepulse to 160 ps/nm. After recombination of the two pulses, they are amplified in the chain of the CPA system including the regenerative Ti:sapphire front end, the Nd:glass preamplifier, and the Nd:glass main amplifier. In the single-pass grating compressor at the end of the laser chain the two pulses are reconstructed. Since here the pulses are recompressed by −200 ps/nm at a bandwidth of about 5 nm full width at half maximum (FWHM) the main pulse is shortened to 7 ps, while the precompressed prepulse is overcompressed to a duration of 200 ps. This setup proved to be a good alternative to the similar concept of [15,16], which uses a stretcher module instead.

Since the two stretched pulses overlap in time because of their strong chirp, a temporal measurement is not possible. To determine the pulse duration of the prepulse $t_p$, the width of the spectrum $\Delta\lambda_p$ is recorded and convoluted with its group delay dispersion $\mathcal{G}_p$, following $t_p$ (ps) $= \Delta\lambda_p$ (nm) $\times\, \mathcal{G}_p$ (ps/nm), while the main pulse duration in the picosecond range is analyzed after compression with a single-shot autocorrelator. To get precise timing on the delay of the double pulse, we used the interference occurring in the spectrum for the differently chirped pulses. An interference peak shows up at the position $x_p$ depending on the time delay of the pulses $t_d$ and the group delay dispersion difference of the pulses $\mathcal{G}_{\text{diff}}$, following $t_d$ (ps) $= x_p$ (nm)$\times\mathcal{G}_{\text{diff}}$ (ps/nm). This yields a resolution of 1 ps for the determination of the time delay. It should be noted that interference effects are not directly influencing the shape of the recompressed pulses.

Because of the traveling-wave pumping, the soft-x-ray laser (SXRL) emission exits the target on one side as shown in Fig. 1. High-energy background radiation from the plasma plume is partly eliminated by a grazing-incidence reflection of the SXRL beam at 6.5° on a polished fused silica substrate with a roughness of 5 nm rms, guiding 20% of the SXRL beam into the spectrometer. The infrared and visible background is suppressed by two 0.8-$\mu$m-thick carbon filters. The SXRL output is imaged via a flat-field gold grating spectrometer with 1200 lines/mm onto a CCD camera at 1.25 m distance to the target.

## III. RESULTS

The pump parameters for highest SXRL output were determined by a delay scan from 20 to 375 ps, a scan of the double-pulse energy ratio between 10% and 70%, and a scan of the total pump energy from 85 to 36 J. The prepulse and

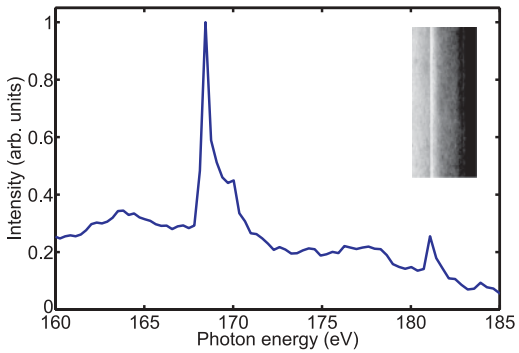


FIG. 2. (Color online) Line profile of the recorded spectrum (see inset) showing the lasing lines of Ni-like Sm at 168.5 eV (7.36 nm) and at 181 eV (6.85 nm).

main pulse durations were set to 200 and 7 ps, respectively, for this study. The contrast level was better than $10^{-6}$, except for an extra pulse of $10^{-3}$ located 900 ps before the double pulse. The spectrum obtained (Fig. 2) shows the lasing of the $4d_{(3/2)}$-$4p_{(3/2)}$ transition at 168.5 eV (7.36 nm) and also the second weaker lasing $4d_{(3/2)}$-$4p_{(1/2)}$ transition at 181 eV (6.85 nm). The line-out of the spectrum is corrected with the transmission of the applied spectrometer.

The vertical divergence of the SXRL was measured to ~6 mrad FWHM, as shown in Fig. 3, clearly showing the directionality of the SXRL. The measured vertical divergence is smaller compared to that of longer-wavelength SXRLs [8,16] owing to reduced refraction effects at the shorter wavelength, and the narrower gain zone for this laser.

The SXRL energy is calculated by integration of the background-corrected counts of the lasing line in the spectrum on the CCD camera chip. The highest SXRL energy obtained is determined to be $\sim 1.6 \pm 0.5$ $\mu$J with respect to the solid angle of the spectrometer, the reflectivity of the gold grating and the fused silica substrate, and the transmission value of the carbon filters. The determined SXRL energy is in agreement with the modeling in [11].

By changing the delay in the Mach-Zehnder interferometer setup, we studied the dependence of the SXRL output on the delay in the double pulse. For this series, the total pump energy was kept constant at ~80 J with ~50% in the prepulse and the delay was varied from 20 to 375 ps. The maximum SXRL

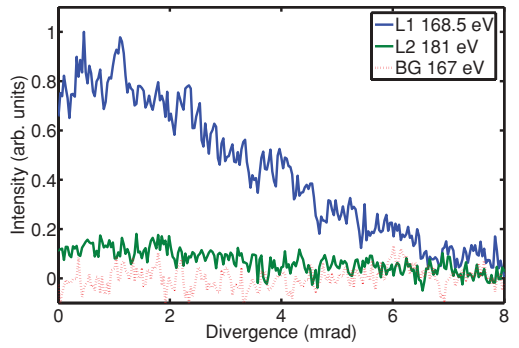


FIG. 3. (Color online) Spatial profile of the two laser lines and the background recorded in the spectrometer, exhibiting a divergence of ~6 mrad FWHM for the full SXRL beam at 168.5 eV in the vertical dimension.

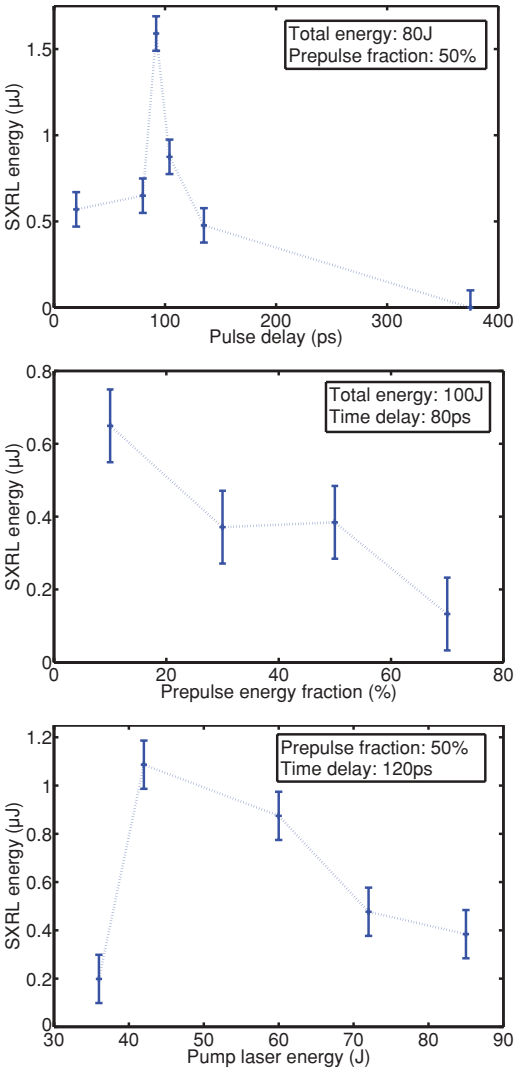


FIG. 4. (Color online) Scan of the double-pulse delay showing a maximum SXRL output for 90 ps with a FWHM of 50 ps, scan of the double-pulse energy ratio showing an increase of the SXRL output with smaller prepulse energy fractions, and scan of the total pump laser energy identifying the pump threshold of 36 J and the optimum at 42 J.

output was found at 90 ps with a FWHM of 50 ps. The small time delay and its narrow window are caused by fast changes in the hydrodynamics of the preplasma [17]. The optimum of 90 ps is close to the result of [11], in which an optimal delay of 130 ps was obtained.

The effect of the double-pulse energy ratio was studied with a total pump energy of ~100 J and a double-pulse delay of ~80 ps. The SXRL output increased by a factor of 5 with variation of the prepulse energy fraction from 70% to 10%. This shows the strong influence of the prepulse energy on the SXRL emission, indicating a maximum at lower prepulse energies toward ~10 J.

The experimental estimation of a total pump energy threshold was done by reducing the total pump energy from 85 down to 36 J. In this case, the prepulse energy fraction was kept constant at ~50% and the delay of the double pulse was ~120 ps. Under these conditions the SXRL output

increased by a factor of 3 with reduction of the energy from 85 to 42 J, where the maximum was found. This shows that a prepulse energy of ∼20 J creates a suitable preplasma condition for this configuration. When the total pump energy was reduced to 36 J, SXRL emission was still observed. At this pump energy the observed emission was five times weaker than at the maximum. The increase of the SXRL output with lower pump energy might be caused by the smaller prepulse energy, confirming the prepulse energy ratio scan in Fig. 4.

## IV. CONCLUSION

The application of double-pulse single-beam non-normal-incidence pumping proves to be a simple and efficient method for the generation of short-wavelength soft-x-ray lasers. Ni-like samarium soft-x-ray lasing at 7.36 nm was achieved at a low total pump energy threshold of 36 J, a value predicted by simulations in [17], and half the total pump energy applied in [11]. This confirms the suitability of the applied pumping scheme for the photon energy region close to 200 eV, with an efficiency of $\sim 4 \times 10^{-8}$. The generation of the double pulse is controlled at the front end and applied for high-energy double pulses up to 100 J without any restraints. With the single-beam single-focusing geometry, the adjustment is fast and stable. The capability of producing a line focus with excellent homogeneity and optimized dimensions at pump laser energies of ∼100 J is demonstrated. The tuning of the pulse front tilt to match the traveling-wave speed along the line focus by the turning of the compressor grating is straightforward and precisely controlled with an autocorrelation mechanism using short double pulses from the Mach-Zehnder interferometer.

The generation of the Ni-like Sm x-ray laser is an important milestone for the feasibility of applying the pumping scheme for higher pumping pulse energies also, which are necessary to obtain soft-x-ray laser wavelengths in the water window [17–19]. With the planned capability of the laser facility PHELIX to bring up to 250 J double-pulse pump laser energy on the target, a Ni-like tungsten soft-x-ray laser at 4.32 nm is conceivable. The reduction of the total pump energy below 40 J for 7 nm lasing satisfies the requirement for installation in high-repetition-rate routine operation at facilities like LASERIX [20] to optimize further the soft-x-ray laser output.

## ACKNOWLEDGMENTS

We would like to thank the teams at PHELIX and LASERIX as well as D. Javorkova and D. Ursescu for their contributions and help. Essential high-energy, high-power laser development relevant for this work benefited from the "Otter" JRA achievements within Laserlab Europe. Experiments of the University Paris Sud 11 team using high-energy pulses at the PHELIX system were supported by the Laserlab Europe Access program. D.Z. is thankful for a "Bourse d'excellence d'Eiffel" grant from Égide.

[1] B. J. MacGowan *et al.*, Phys. Rev. Lett. **65**, 420 (1990).
[2] J. Zhang *et al.*, Science **276**, 1097 (1997).
[3] R. Smith, G. J. Tallents, J. Zhang, G. Eker, S. McCabe, G. J. Pert, and E. Wolfrum, Phys. Rev. A **59**, 47(R) (1999).
[4] H. Daido *et al.*, J. Opt. Soc. Am. B **16**, 2295 (1999).
[5] P. V. Nickles, V. N. Shlyaptsev, M. Kalachnikov, M. Schnrer, I. Will, and W. Sandner, Phys. Rev. Lett. **78**, 2748 (1997).
[6] J. Dunn, Y. Li, A. L. Osterheld, J. Nilsen, J. R. Hunter, and V. N. Shlyaptsev, Phys. Rev. Lett. **84**, 4834 (2000).
[7] R. Keenan, J. Dunn, P. K. Patel, D. F. Price, R. F. Smith, and V. N. Shlyaptsev, Phys. Rev. Lett. **94**, 103901 (2005).
[8] J. J. Rocca, Y. Wang, M. A. Larotonda, B. M. Luther, M. Berrill, and D. Alessi, Opt. Lett. **30**, 2581 (2005).
[9] M. Gruenig, C. Imesch, F. Staub, and J. E. Balmer, Opt. Commun. **282**, 267 (2009).
[10] T. Kawachi, A. Sasaki, M. Tanaka, M. Kishimoto, N. Hasegawa, K. Nagashima, M. Koike, H. Daido, and Y. Kato, Phys. Rev. A **69**, 033805 (2004).
[11] R. E. King *et al.*, Phys. Rev. A **64**, 053810 (2001).
[12] V. Bagnoud *et al.*, Appl. Phys. B (2009), doi:10.1007/s00340-009-3855-7.
[13] D. Zimmer, B. Zielbauer, V. Bagnoud, U. Eisenbarth, D. Javorkova, and T. Kuehl, Opt. Express **16**, 10398 (2008).
[14] J.-C. Chanteloup *et al.*, J. Opt. Soc. Am. B **17**, 151 (2000).
[15] T. Kawachi *et al.*, Appl. Opt. **42**, 2198 (2003).
[16] D. Zimmer, B. Zielbauer, M. Pittman, O. Guilbaud, J. Habib, S. Kazamias, D. Ros, V. Bagnoud, and T. Kuehl, Opt. Lett. **35**, 450 (2010).
[17] G. J. Pert, Phys. Rev. A **73**, 033809 (2006).
[18] G. J. Pert, Phys. Rev. A **75**, 023808 (2007).
[19] G. J. PertPhys. Rev. A **75**, 063814 (2007).
[20] F. Ple, M. Pittman, G. Jamelot, and J. P. Chambaret, Opt. Lett. **32**, 238 (2007).